Gauge-invariant smearing and matrix correlators using Wilson fermions at $\beta=6.2$

C. R. Allton* and C. T. Sachrajda
Physics Department, University of Southampton, Southampton SO9 5NH, United Kingdom

R. M. Baxter, S. P. Booth, K. C. Bowler, S. Collins, D. S. Henty, R. D. Kenway, B. J. Pendleton, D. G. Richards, J. N. Simone, A. D. Simpson, and B. E. Wilkes
Department of Physics, University of Edinburgh, Edinburgh EH9 3JZ, Scotland

C. Michael
Department of Applied Mathematics and Theoretical Physics (DAMTP), University of Liverpool, Liverpool L69 3BX, United Kingdom

(UKQCD Collaboration)
(Received 8 January 1993)

We present an investigation of gauge-invariant smearing for Wilson fermions in quenched lattice QCD on a $24^3\times 48$ lattice at $\beta=6.2$. We demonstrate a smearing algorithm that allows a substantial improvement in the determination of the baryon spectrum obtained using propagators smeared at both source and sink, at only a small computational cost. We investigate the matrix of correlators constructed from local and smeared operators, and are able to expose excited states of both the mesons and baryons.

PACS number(s): 12.38.Gc, 11.15.Ha

I. INTRODUCTION

The use of "smeared" interpolating fields to expose more clearly the leading behavior of Euclidean correlators has become standard practice in lattice gauge simulations. The extended sources first suggested in [1,2] comprise a sum of δ functions on the source time slice and therefore are not gauge covariant. These sources give an improved signal for small Euclidean times, but lead to increased statistical noise at large times. The noise problem can be cured by fixing to Coulomb gauge on the source time slice, and the resulting "cube" [3] and "wall" [4] sources, and variants thereof [5,6], have been used in many areas of lattice QCD phenomenology. A more ambitious approach is to measure Coulomb-gauge wave functions, and to use these as sources to improve the overlap with the ground state [7–9].

When fixing to a smooth gauge such as the Coulomb or Landau gauge, one must be careful that ambiguities in the gauge-fixing condition [10] do not affect the final result. In this paper we avoid the gauge-fixing problem through the use of gauge-covariant sources [11,12].

The plan of this paper is as follows. We begin by comparing effective masses obtained from local sinks with those from Wuppertal scalar-propagator smeared sinks [11]. We introduce a variant of the alternative iterative Wuppertal scheme which enables us to achieve similar results to scalar propagator smearing, but at a much lower cost in computer time. Using this scheme, we perform detailed measurements of the hadron spectrum and the pseudoscalar decay constant using local propagators (LL), propagators smeared at the source only (LS), at the sink only (SL), and at both source and sink (SS). Finally, we investigate the 2×2 matrix of correlators formed from propagators computed with the four source-sink combinations, and by diagonalizing this matrix are able to isolate the first excited state in the various meson and baryon channels.

II. EUCLIDEAN CORRELATORS

In lattice field theory, masses and matrix elements are obtained from the asymptotic exponential decay of two-point correlation functions of the form

$$c_{\mathcal{O}\tilde{\mathcal{O}}}(t)=\sum_{\mathbf{x}}\langle \mathcal{O}(\mathbf{x},t)\tilde{\mathcal{O}}^{\dagger}(\mathbf{0},0)\rangle e^{-i\mathbf{p}\cdot\mathbf{x}}\,, \tag{1}$$

where the operator $\tilde{\mathcal{O}}^{\dagger}$ at the source $(\mathbf{0},0)$ has the appropriate quantum numbers to create the hadron h of interest. This hadron is destroyed at the sink by an appropriate operator $\mathcal{O}(\mathbf{x},t)$. Inserting a complete set of eigenstates of the Hamiltonian, we find

$$c_{\mathcal{O}\tilde{\mathcal{O}}}(t)=\frac{\langle 0|\mathcal{O}(0)|h_0(\mathbf{p})\rangle\langle h_0(\mathbf{p})|\tilde{\mathcal{O}}^{\dagger}(0)|0\rangle}{2E_0(\mathbf{p})}e^{-E_0(\mathbf{p})t}A(t)\,, \tag{2}$$

where the correction $A(t)$ to the asymptotic behavior is

$$A(t)=1+\sum_{n=1}^{\infty}\frac{E_0(\mathbf{p})}{E_n(\mathbf{p})}\frac{\langle 0|\mathcal{O}(0)|h_n(\mathbf{p})\rangle\langle h_n(\mathbf{p})|\tilde{\mathcal{O}}^{\dagger}(0)|0\rangle}{\langle 0|\mathcal{O}(0)|h_0(\mathbf{p})\rangle\langle h_0(\mathbf{p})|\tilde{\mathcal{O}}^{\dagger}(0)|0\rangle}\times e^{-[E_n(\mathbf{p})-E_0(\mathbf{p})]t}\,. \tag{3}$$

*Present address: Dipartimento di Fisica, Università di Roma I, La Sapienza, 00185 Roma, Italy.

$|h_0(\mathbf{p})\rangle$ is the lightest hadron state with three-momentum $\mathbf{p}$ that can be created by $\tilde{\mathcal{O}}^\dagger$, and $|h_n(\mathbf{p})\rangle$ is its nth excited state. With a suitable choice of $\mathcal{O}$ and $\tilde{\mathcal{O}}$, we hope to enhance the matrix elements between the vacuum and the lightest state, so that the coefficients of the nonleading exponentials of Eq. (3) are reduced, and the asymptotic behavior $[A(t)\rightarrow 1]$ is reached for small t, where statistical errors are small.

III. GAUGE-INVARIANT SMEARING

A. Computational details

Our simulations were performed on a $24^3\times 48$ lattice at $\beta=6.2$ using quenched Wilson fermions, with a hopping parameter $\kappa=0.152$. This corresponds to a pseudoscalar meson mass of approximately 600 MeV if we set the scale from the string tension ($a^{-1}\sim 2.73(5)$ GeV [13]), or from m_ρ. The configurations were generated on a Meiko i860 Computing Surface, and the propagators on a Thinking Machines CM-200, both at Edinburgh.

B. Wuppertal smearing

The Wuppertal scalar-propagator smeared source [11], $S(\mathbf{x}',\mathbf{0})$, is given by the solution of the three-dimensional Klein-Gordon equation

$$K(\mathbf{x},\mathbf{x}')S(\mathbf{x}',\mathbf{0})=\delta_{\mathbf{x},\mathbf{0}}\ , \tag{4}$$

where

$$K(\mathbf{x},\mathbf{x}')=\delta_{\mathbf{x},\mathbf{x}'}-\kappa_S\sum_\mu\{\delta_{\mathbf{x}',\mathbf{x}-\hat{\mu}}U_\mu^\dagger(\mathbf{x}-\hat{\mu}) +\delta_{\mathbf{x}',\mathbf{x}+\hat{\mu}}U_\mu(\mathbf{x})\}\ . \tag{5}$$

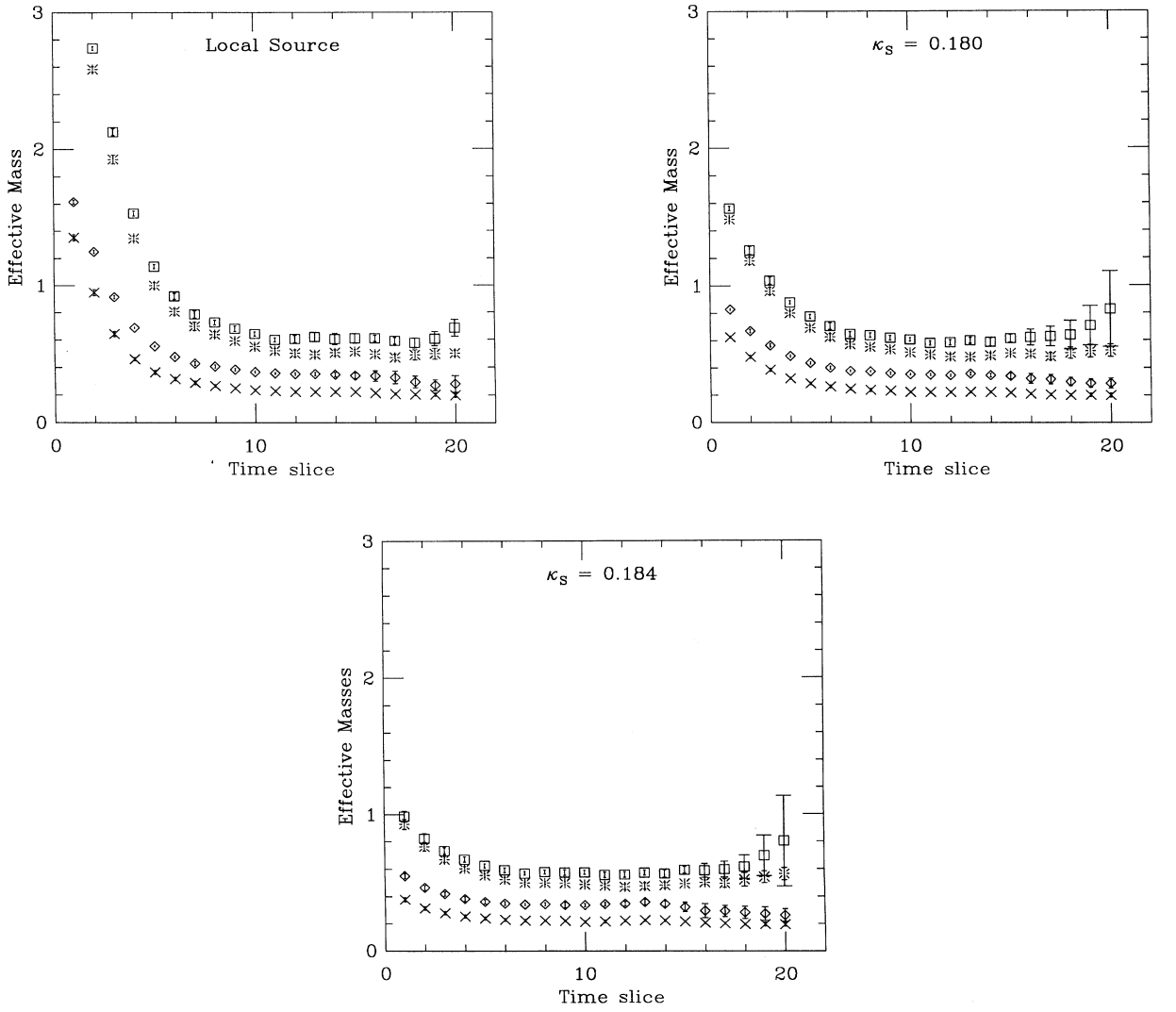

FIG. 1. The effective masses of the pseudoscalar (crosses), vector (diamonds), nucleon (bursts), and △ (squares) on an ensemble of seven configurations, using propagators calculated with a local source, and with Wuppertal scalar-propagator smeared sources at $\kappa_S=0.180$ and $\kappa_S=0.184$. A local sink is used in each case.

This leads to a so-called "shell-model" wave function [5], in which each quark is effectively localized about the origin in a region of radius r controlled by the scalar hopping parameter κ_S. The rms radius r is defined by

$$r^2=\frac{\sum_{\mathbf{x}}|\mathbf{x}|^2|S(\mathbf{x},0)|^2}{\sum_{\mathbf{x}}|S(\mathbf{x},0)|^2} . \tag{6}$$

For the initial investigation of the dependence of the effective masses on the smearing radius, quark propagators were computed on an ensemble of seven configurations using Wuppertal smeared sources at $\kappa_S=0.180$ and 0.184, corresponding to $r\simeq 2$ and $r\simeq 4$, respectively. The effective masses of the pseudoscalar, vector, nucleon, and Δ are shown in Fig. 1, together with the results for a point source on the same ensemble of configurations. The lightest state in each channel is isolated nearer the origin with increasing smearing radius; we will investigate below whether this yields an improvement in the statistical uncertainty on the hadron mass determined from a correlated fit to the corresponding propagator.

The computational overhead of Wuppertal smearing at the source is relatively small compared with the work required in the computation of the propagator. However, the overhead is significant when the propagator is smeared at the sink, as is generally required to realize an improvement in the determination of matrix elements, since the smearing algorithm must be implemented on every time slice, and for every spin component. Indeed, for $\kappa_S=0.184$, the computational effort required to smear at the sink is comparable with that required to compute the propagator, and larger values of the smearing radius are prohibitively expensive.

C. Jacobi smearing

An alternative smeared source can be obtained by solving Eq. (4) as a power series in κ_S, stopping at some finite power N. This can be achieved easily using Jacobi iteration. When κ_S is smaller than some critical value, the power series converges and one recovers the scalar propagator. For sufficiently large κ_S, the series diverges but provides a valid smeared source for any choice of N. A similar iterative scheme has been used by the Wuppertal group [11,14].

We can construct a smearing function of given radius, r, for various choices of $\{N,\kappa_S\}$. However, there is a minimum N required to achieve a particular radius. Typical source functions with $r\simeq 4$, for $\{N=50,\ \kappa_S=0.250\}$, $\{N=90,\ \kappa_S=0.190\}$ together with the Wuppertal source function at $\kappa_S=0.184$, are shown in Fig. 2. For this radius, $N=50$ is close to minimal. The Jacobi source function can be generated in considerably less computer time than the Wuppertal source function; approximately a factor of 10 less at this radius. Furthermore, the truncation of the Jacobi series suppresses fluctuations in the norm and in r between configurations; hence there is some additional advantage in taking the minimum value of N.

From the spectral representation (2), it is easy to see that, when $\mathcal{O}=\tilde{\mathcal{O}}$, correlators obtained from propagators smeared at the source (LS) and those obtained from propagators smeared at the sink with local sources (SL) are equal in the limit that the path integral over the gauge fields is done exactly. However, for a finite sample of configurations, sink smearing leads to more statistical

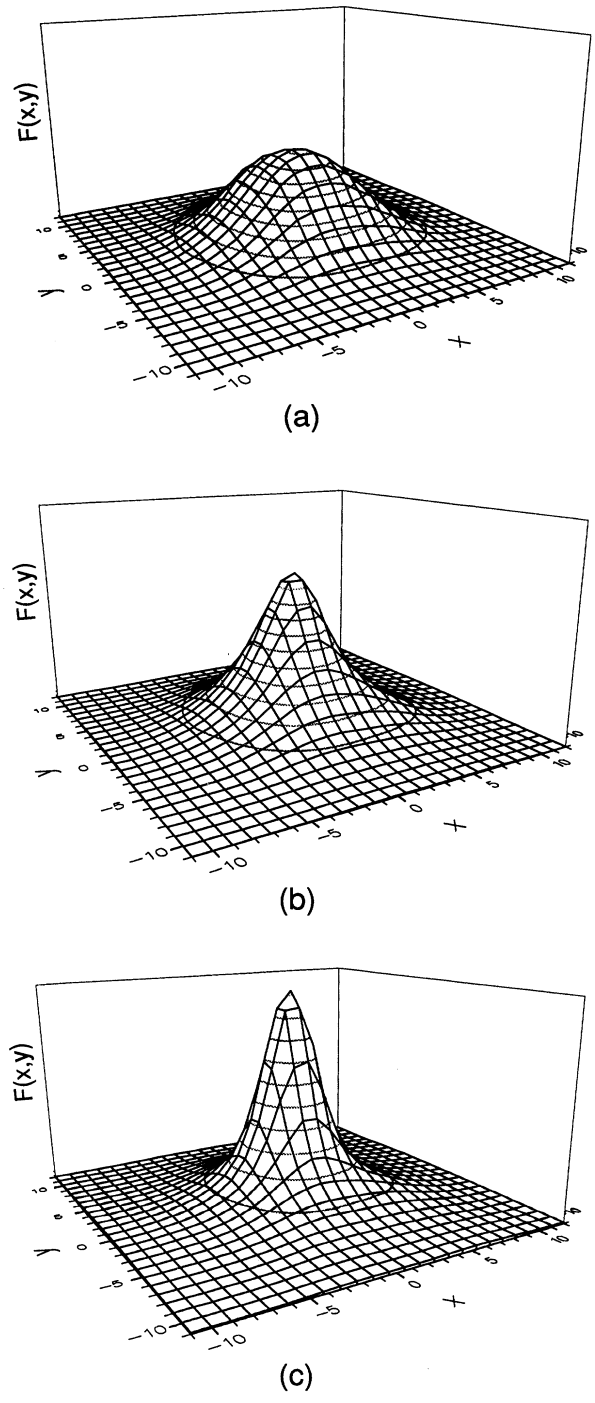

FIG. 2. The smearing functions $F(x,y)=\sqrt{|S|^2}|_{z=0}$, normalized to unit volume, on a $24^3\times 48$ lattice using (a) Jacobi smearing with $\kappa_S=0.250$, $N=50$, (b) Jacobi smearing with $\kappa_S=0.190$, $N=90$, and (c) Wuppertal smearing with $\kappa_S=0.184$.

noise because of fluctuations in the gauge fields forming the sinks on different time slices. We found that for radii greater than 4, this noise becomes unacceptably high, though a quantitative comparison of SL and LS results for hadron masses must await the correlated fits to the data presented below. Nevertheless, the remainder of this paper will concentrate on results with $r \simeq 4$ on the same 18 configurations which were studied in [13], using a Jacobi source function with $\kappa_S = 0.250$, $N = 50$.

To optimize the onset of asymptotic behavior, we look at propagators smeared both at the source and the sink (SS). The effective masses of the pseudoscalar, vector, nucleon, and Δ obtained using the LL, LS, SL, and SS propagators are shown in Fig. 3.

IV. HADRON MASSES

To quantify the preceding discussion, we present in Table I the masses in lattice units of the pseudoscalar, vector, nucleon, and Δ using the LL, LS, SL, and SS propagators, together with the corresponding time ranges used for the fits. All fits are performed using the full covariance matrix, with the errors extracted using a bootstrap analysis [15]. For each of the four source-sink combinations, the time range was chosen by requiring that the fit be stable under the removal from the fitting range of the time slice closest to the source. The length of the fitting range is constrained by the number of configurations. Here we fit to the average of the appropriate forward and backward propagators, in contrast to [13] where we fitted to the forward and backward propagators independently.

As expected, the mass estimates obtained using the SL propagators are subject to substantially larger errors than those obtained using the LS propagators, even though the fitting range used is the same. The improvement in the determination of the baryon masses through the use of smeared sources and sinks is substantial. It is possible

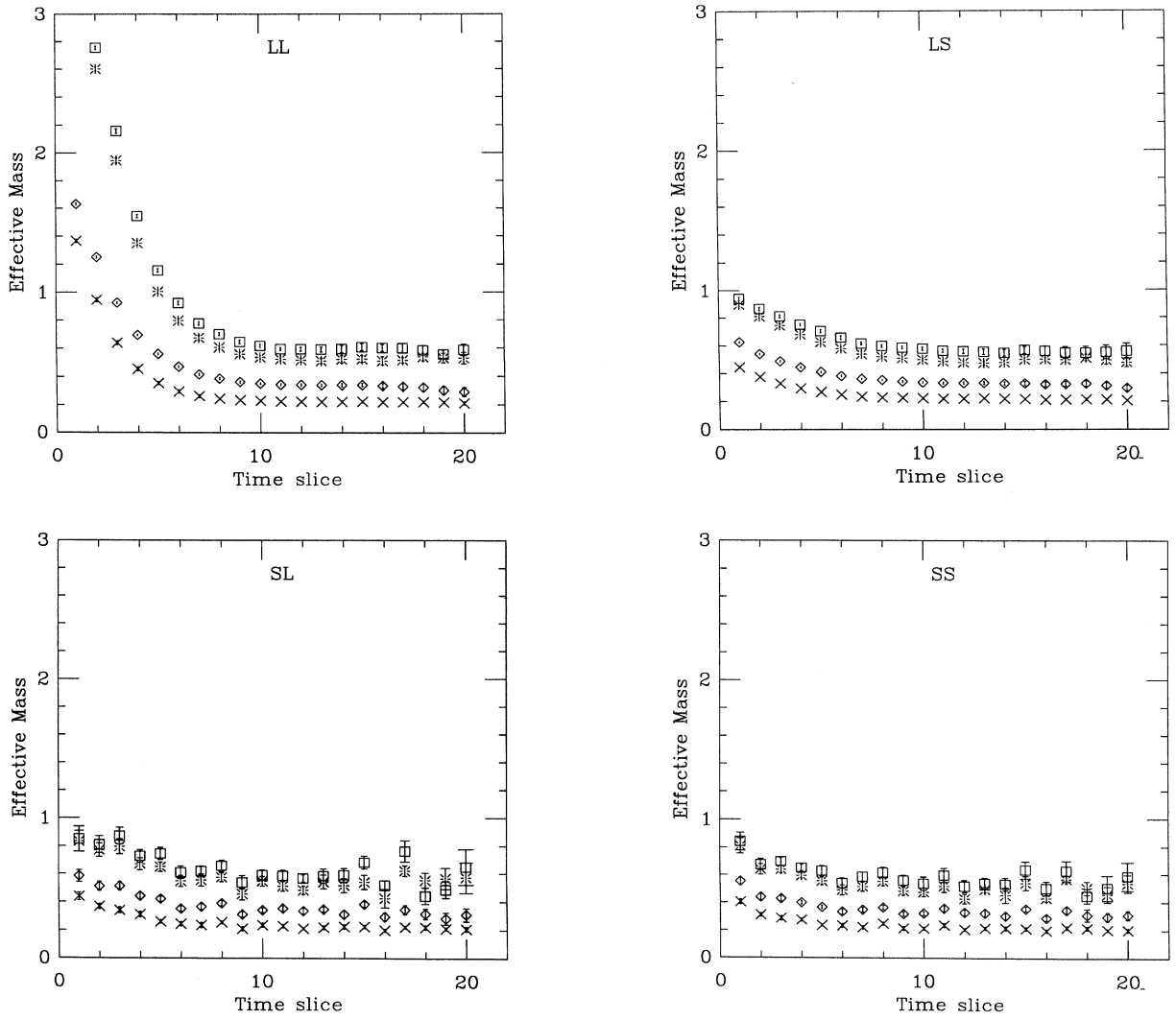

FIG. 3. The effective masses of the pseudoscalar (crosses), vector (diamonds), nucleon (bursts), and $\triangle$ (squares), computed using the LL, LS, SL, and SS propagators, with a Jacobi smearing algorithm as discussed in the text.

TABLE I. The estimates of baryon and meson masses using LL, SL, LS, and SS propagators with a Jacobi smearing algorithm comprising 50 iterations at $\kappa_S=0.250$. Also shown in parentheses is the time range used in each fit.

	LL	SL	LS	SS
m_P	0.223^{+5}_{-6}(12–16)	0.220^{+12}_{-8}(11–16)	0.219^{+9}_{-4}(11–16)	0.220^{+7}_{-7}(9–12)
m_V	0.341^{+10}_{-7}(12–16)	0.356^{+21}_{-13}(11–16)	0.327^{+8}_{-7}(11–16)	0.327^{+9}_{-8}(9–12)
m_N	0.510^{+23}_{-10}(12–16)	0.507^{+31}_{-24}(11–16)	0.495^{+12}_{-12}(11–16)	0.495^{+9}_{-10}(7–12)
m_Δ	0.595^{+15}_{-16}(12–16)	0.593^{+32}_{-16}(11–16)	0.567^{+12}_{-17}(11–16)	0.559^{+9}_{-10}(7–12)

that the study of a larger sample of configurations would lead to a still more marked improvement through the ability to perform a fit to the full covariance matrix for the SS correlators over a larger fitting range than that quoted in Table I.

A recent analysis [16] of the hadron spectrum obtained using both wall sources and Wuppertal sources suggests that there is a systematic difference in the baryon masses in the two cases, and that this difference is particularly noticeable in the determination of the Δ mass. To determine whether such discrepancies exist in our data, Table II shows bootstrap analyses of the Δ mass differences for the various combinations of sources and sinks, using the time ranges of Table I. Any discrepancies are at most a 2σ effect, and furthermore appear to depend only on the interpolating field used at the source, and not on that used at the sink. Since the expectation values of the LS and SL correlators should be identical in the limit of an infinite number of configurations, we attribute the discrepancies to limited statistics.

V. PSEUDOSCALAR DECAY CONSTANT

The hope of an improvement in the determination of hadronic matrix elements provides strong motivation for the use of smeared operators. In this section, we take the pseudoscalar decay constant f_P to typify a matrix element that can be computed from two-point functions.

For a pseudoscalar at rest, the decay constant is related to the matrix element of the (local) axial vector current by

$$\langle 0|A^4_{\rm L}(0)|P\rangle = f_P m_P \ , \tag{7}$$

where $A^\mu_{\rm L}$ is the axial operator $\bar{q}\gamma_5\gamma_\mu q$. For the following discussion, we introduce the amplitudes $Z_{\rm L(S)}$ defined by

$$\langle 0|P_{\rm L(S)}(0)|P\rangle = Z_{\rm L(S)} m_P \ , \tag{8}$$

where P is the pseudoscalar operator $\bar{q}\gamma_5 q$, and the L and S subscripts denote quantities constructed using local and smeared operators, respectively.

TABLE II. The entries represent the Δ mass differences obtained by subtracting the source-sink combination on the top from that on the left.

	$m_{\rm LL}$	$m_{\rm SL}$	$m_{\rm LS}$	$m_{\rm SS}$
$m_{\rm LL}$	0.0	0.002^{+11}_{-25}	0.028^{+15}_{-17}	0.036^{+16}_{-18}
$m_{\rm SL}$		0.0	0.026^{+31}_{-20}	0.035^{+30}_{-20}
$m_{\rm LS}$			0.0	0.008^{+19}_{-18}
$m_{\rm SS}$				0.0

We find that the cleanest determination of f_P using local sources and sinks [15] is obtained by fitting to the ratio

$$\frac{\sum_{\mathbf{x}}\langle A^4_{\rm L}(\mathbf{x},t)P^\dagger_{\rm L}(0)\rangle}{\sum_{\mathbf{x}}\langle P_{\rm L}(\mathbf{x},t)P^\dagger_{\rm L}(0)\rangle} \sim \frac{f_P}{Z_{\rm L}}\tanh m_P(T/2-t) \ , \tag{9}$$

where T is the temporal extent of the lattice, and $Z_{\rm L}$ and m_P are determined from the fit to the pseudoscalar correlator. Using the fitting range of Table I (12–16), we find

$$f_P = 0.066^{+1}_{-3} \ , \tag{10}$$

where the result is expressed in lattice units. The determination through the correlator $\langle P_{\rm L}(\mathbf{x},t)A^{4\dagger}_{\rm L}(0)\rangle$ has larger statistical errors.

From propagators computed with both smeared and local sources and sinks, we can extract f_P from the ratio

$$\frac{\sum_{\mathbf{x}}\langle A^4_{\rm L}(\mathbf{x},t)P^\dagger_{\rm S}(0)\rangle}{\sum_{\mathbf{x}}\langle P_{\rm S}(\mathbf{x},t)P^\dagger_{\rm S}(0)\rangle} \sim \frac{f_P}{Z_{\rm S}}\tanh m_P(T/2-t) \ , \tag{11}$$

where $Z_{\rm S}$ and m_P are determined from the fit to the appropriate SS correlator. Using the time range 11 to 16 for the fit to Eq. (11), and the range 9 to 12 for the fit to the SS correlator, we obtain

$$f_P = 0.065^{+3}_{-4} \ . \tag{12}$$

The determinations of f_P using the two methods are consistent. That we see no improvement using the smeared propagators may arise from the inability to exploit the full time range in the correlated fits due to the limited statistical sample. However, we note that the statistical error on f_P using the local propagators is already small, and that we may be close to the minimum achievable statistical error. The improvement in the determination of the baryon masses through the use of smeared correlators encourages us to believe that there may be a corresponding reduction in the uncertainty on baryon matrix elements.

VI. MATRIX CORRELATORS

By studying the matrix of correlators formed from the interpolating fields constructed using smeared and local sources and sinks, we can attempt to extract masses for the first excited state. We begin this section with a discussion of the case of a general 2×2 matrix of correlators.

A. Method

Consider the two operators, $\mathcal{O}_a$ and $\mathcal{O}_b$, having the same quantum numbers, and a basis of states,

$$|h_n(\mathbf{p})\rangle, \quad n=0,\ 1,2,\ldots . \tag{13}$$

We define the 2×2 matrix $C(t)$ of time-sliced correlators by

$$C(t)=\begin{bmatrix} c_{aa}(t) & \omega c_{ab}(t) \\ \omega c_{ba}(t) & \omega^2 c_{bb}(t) \end{bmatrix},$$

with

$$c_{ij}(t)=\sum_{\mathbf{x}} \langle 0|\mathcal{O}_i(\mathbf{x},t)\mathcal{O}_j^{\dagger}(\mathbf{0},0)|0\rangle e^{-i\mathbf{p}\cdot\mathbf{x}}, \tag{14}$$

where ω is the arbitrary relative normalization of the operators $\mathcal{O}_b$ and $\mathcal{O}_a$. Inserting a complete set of states in Eq. (14), we obtain

$$C(t)=\sum_{n\geq 0} e^{-E_n(\mathbf{p})t}\begin{bmatrix} |a_n|^2 & a_n^* b_n \omega \\ b_n^* a_n \omega & |b_n|^2\omega^2 \end{bmatrix}, \tag{15}$$

where

$$a(b)_n=\frac{1}{\sqrt{2E_n(\mathbf{p})}}\langle 0|\mathcal{O}_{a(b)}|h_n(\mathbf{p})\rangle . \tag{16}$$

We will now discuss two methods for studying the matrix $C(t)$ [17].

1. Diagonalization of transfer matrix

Consider the eigenvalue equation

$$C(t)u=\lambda(t,t_0)C(t_0)u , \tag{17}$$

for fixed $t_0<t$. If the system comprises only two independent states, then the eigenvalues, $\lambda_+(t,t_0)$ and $\lambda_-(t,t_0)$, of Eq. (17) are

$$\begin{aligned} \lambda_+(t,t_0)&=e^{-(t-t_0)E_0}, \\ \lambda_-(t,t_0)&=e^{-(t-t_0)E_1}. \end{aligned} \tag{18}$$

The two states are separated exactly, and the coefficients in Eq. (18) grow exponentially with t_0. In general, where there are more than two states, we expect only two states to be dominant for sufficiently large t; the coefficients of the contributions of the higher states are suppressed. Hence ideally we wish to study $\lambda(t,t_0)$ for t_0 as large as possible. However, the increase in the noise in the data far from the source generally requires that we choose t_0 close to the origin.

We consider a fixed basis of operators by introducing the matrix of eigenvectors $M(t)$ which diagonalizes $C(t_0)^{-1}C(t)$ at $t=t_0+1$. In a regime in which effectively we have only two states, the diagonal elements of the matrix

$$M(t_0+1)^{-1}C(t_0)^{-1}C(t)M(t_0+1) \tag{19}$$

are independent of t_0, and equivalent to the eigenvalues of $C(t_0)^{-1}C(t)$.

2. Diagonalization of $C(t)$

We can compute the eigenvalues, $\chi_+(t,\omega)$ and $\chi_-(t,\omega)$, of $C(t)$ directly, and at large times, t, obtain

$$\begin{aligned} \chi_+(t,\omega)&=f_+(\omega,a_i,b_i)e^{-E_0(\mathbf{p})t}[1+g_+(\omega,a_i,b_i)O(e^{-\Delta E_1(\mathbf{p})t})], \\ \chi_-(t,\omega)&=f_-(\omega,a_i,b_i)e^{-E_1(\mathbf{p})t}[1+g_-(\omega,a_i,b_i)O(e^{-\Delta\tilde{E}(\mathbf{p})t})], \end{aligned} \tag{20}$$

where

$$\begin{aligned} \Delta E_n(\mathbf{p})&=E_n(\mathbf{p})-E_0(\mathbf{p}), \\ \Delta\tilde{E}(\mathbf{p})&=\min[E_1(\mathbf{p})-E_0(\mathbf{p}),E_2(\mathbf{p})-E_1(\mathbf{p})] . \end{aligned} \tag{21}$$

As in method 1, $\chi_+(t,\omega)$ and $\chi_-(t,\omega)$ are dominated by the ground state and first excited state, respectively. However, even when there are only two states, corrections to the leading behavior of the eigenvalues remain. The coefficients of these corrections depend on the arbitrary parameter ω and, since we diagonalize $C(t)$ at each time slice, these coefficients are not positive definite. We will exploit the dependence on ω to seek cancellations between the contributions from higher states, and hence extend the plateau region in the effective mass closer to the source.

Such an approach has clear dangers. In particular, the effective masses can approach their asymptotic values either from above or from below as we vary ω. However, we observe that for sufficiently large times the excited state contributions to Eq. (20) will be negligible, and thus the effective masses derived from $\chi_+(t,\omega)$ and $\chi_-(t,\omega)$ must be insensitive to ω.

B. Results

Here we consider $\mathcal{O}_a$ and $\mathcal{O}_b$ to be the local ($\mathcal{O}_L$) and smeared ($\mathcal{O}_S$) interpolating fields, respectively, with $C(t)$ computed at zero spatial momentum. In Fig. 4, we show the effective masses of the first excited states derived from the eigenvalues $\lambda_-(t,t_0)$ for the pseudoscalar, vector, nucleon, and Δ channels, with $t_0=1$. We find increasing t_0 has no effect on the effective masses except to increase the statistical error. Also shown are the effective masses derived from the smaller diagonal elements of

$$M(t_0+1)^{-1}C(t_0)^{-1}C(t)M(t_0+1), \quad \text{for } t_0=4 ;$$

the effective masses for $t_0=5$ and $t_0=6$ are consistent. We see that the effective masses lie on those derived from $\lambda_-(t,\ t_0=1)$, and conclude that two states are effectively dominant for $t_0\geq 4$.

In Fig. 5, we show the effective masses of the first excited states derived from $\chi_-(t,\omega)$ for the pseudoscalar, vector, nucleon, and Δ channels, at $\omega=10\omega_0$, ω_0, and $0.1\omega_0$, where

$$\omega_0=\left[\frac{C_{\rm LL}(t=12)}{C_{\rm SS}(t=12)}\right]^{1/2}. \tag{22}$$

For each channel there is a region in t for which the effective masses coincide for all ω. As noted above, this can be taken as a signal for the first excited state. The plateau region in the effective masses appears to extend closer to the source as ω decreases. We attribute this to cancellations between contributions of the higher excited states to $\chi_-(t,\omega)$.

Figure 6 shows the effective masses of the first excited states using method 1, and using method 2 at an approximately optimal value of ω. The two methods yield consistent plateaus in the pseudoscalar, vector, and nucleon channels, and using method 2 we obtain

$$\begin{aligned}\tilde{m}_P(5\text{–}8)&=0.93^{+6}_{-13}\,,\\ \tilde{m}_V(5\text{–}8)&=0.90^{+3}_{-4}\,,\\ \tilde{m}_N(6\text{–}9)&=1.02^{+6}_{-6}\,,\end{aligned} \tag{23}$$

where the fitting range is shown in parentheses. Our fitting procedure is as follows. We pick a value of ω which provides the largest plateau region in the effective mass of the first excited state. We then perform a correlated fit to the eigenvalue $\chi_-(t,\omega)$, using a fitting range such that the fit is insensitive, within statistical errors, to the addition of the time slice closer to the source. We estimate the systematic errors by looking at the variation in the central value of the mass as we vary ω about the optimal value, keeping the time range fixed; we find the sys-

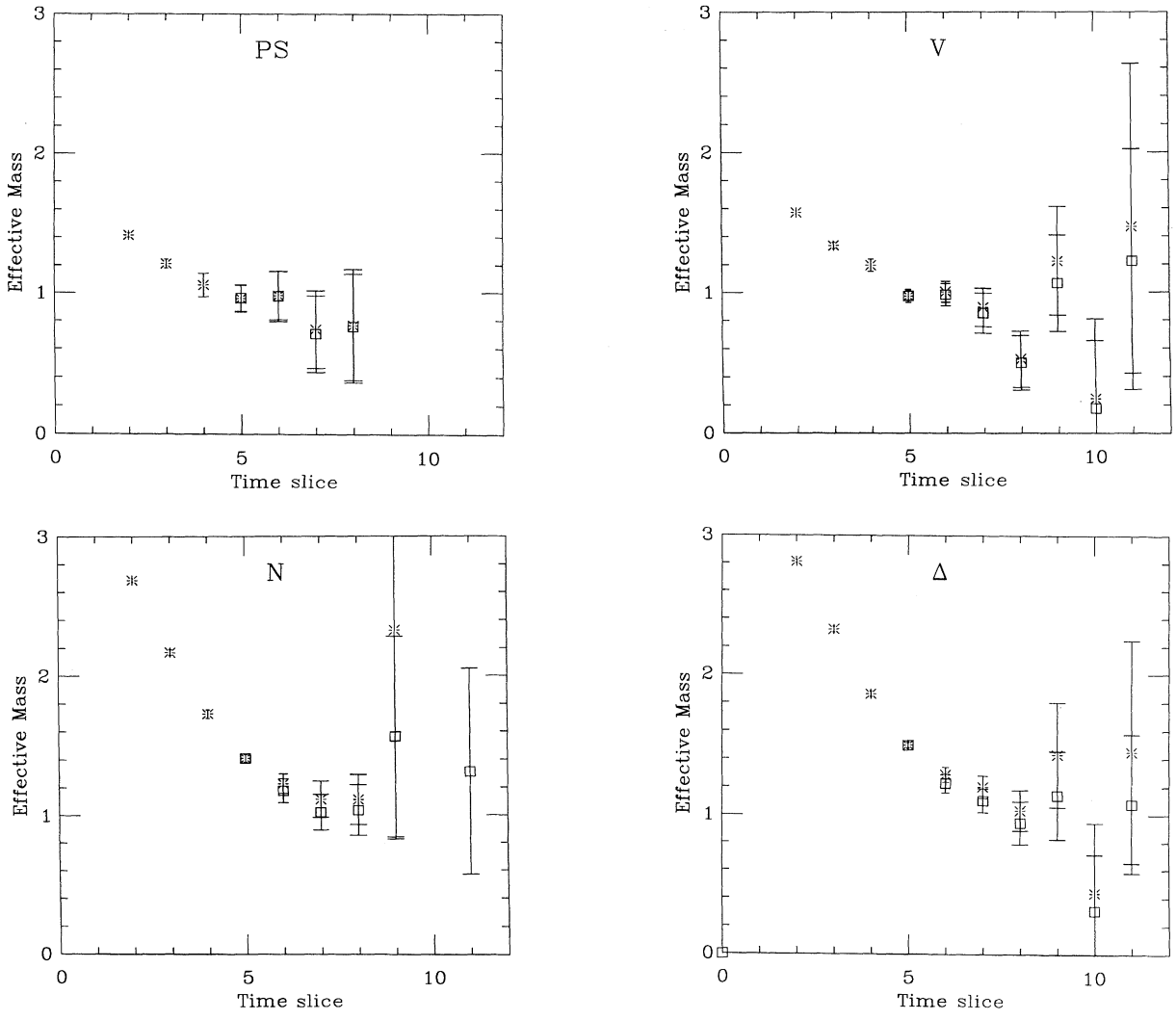

FIG. 4. The effective masses of the first excited states in the pseudoscalar, vector, nucleon, and $\triangle$ channels, derived from $\lambda_-(t,t_0)$, for $t_0=1$ (bursts). Also shown are the effective masses derived from the smaller diagonal elements of $M(t_0+1)^{-1}C(t_0)^{-1}C(t)M(t_0+1)$, for $t_0=4$ (squares).

tematic errors to be of order 5%.

There is no clear plateau in the effective mass in the Δ channel using method 1. However, using method 2 we obtain

$$\tilde{m}_{\Delta}(6\text{–}9)=1.02^{+5}_{-3}\ . \tag{24}$$

We find that the masses of the first excited states are more than twice those of the corresponding ground states. The quark mass employed in our investigation is somewhat less than that of the strange quark. The measured ratios are therefore considerably larger than the corresponding experimental ratios for hadrons consisting entirely of strange quarks, e.g., $m_{\Omega(2250)^-}/m_{\Omega^-}\simeq 1.35$, $m_{\phi(1680)}/m_{\phi(1020)}\simeq 1.65$. If this is disappointing, it should be noted that all our computed values of the first excited state masses are $O(1)$. Since the mass differences between these states and the corresponding ground states arise from radial excitations, the discretization errors may be substantial. Furthermore, unexpectedly large values for the masses of the excited states have been observed in other simulations [18]. We conclude this section by remarking that an investigation of the larger eigenvalue, $\lambda_+(t,t_0)$, of method 1 yields similar results for the ground-state masses to those obtained from the analysis of the SS correlators.

VII. CONCLUSIONS

We have demonstrated a gauge-invariant smearing algorithm that provides a considerable improvement in the determination of baryon masses. Though we see some discrepancy between the baryon masses obtained using local sources and those obtained using smeared sources, it is very small, and we attribute it to the limited statistics.

An investigation of the 2×2 matrices of correlators formed from the LL, SL, LS, and SS propagators allows

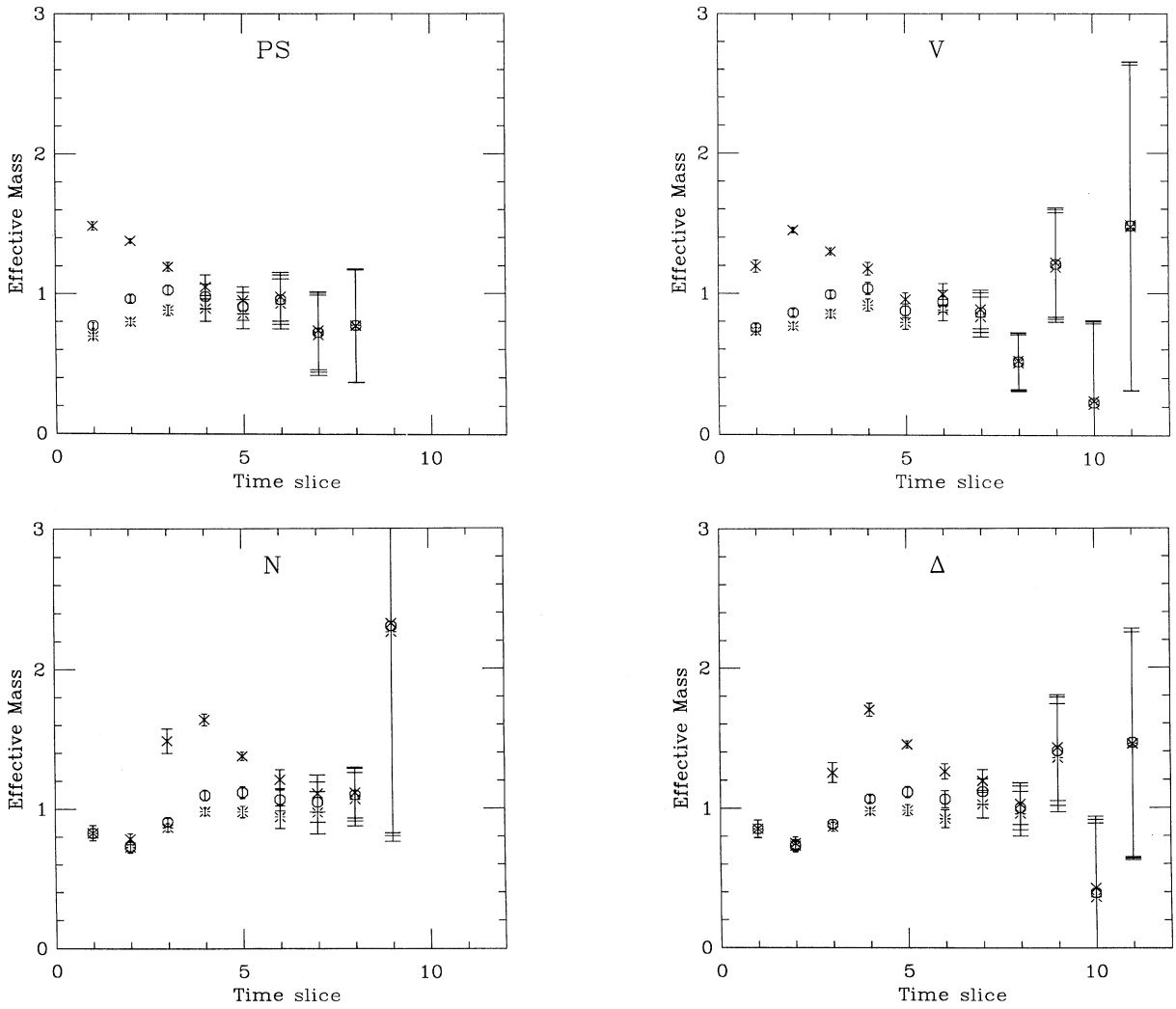

FIG. 5. The effective masses of the first excited states in the pseudoscalar, vector, nucleon, and $\triangle$ channels, derived from $\chi_-(t,\omega)$, for $\omega=\omega_0$ (circles), $\omega=10\omega_0$ (crosses), and $\omega=0.1\omega_0$ (bursts).

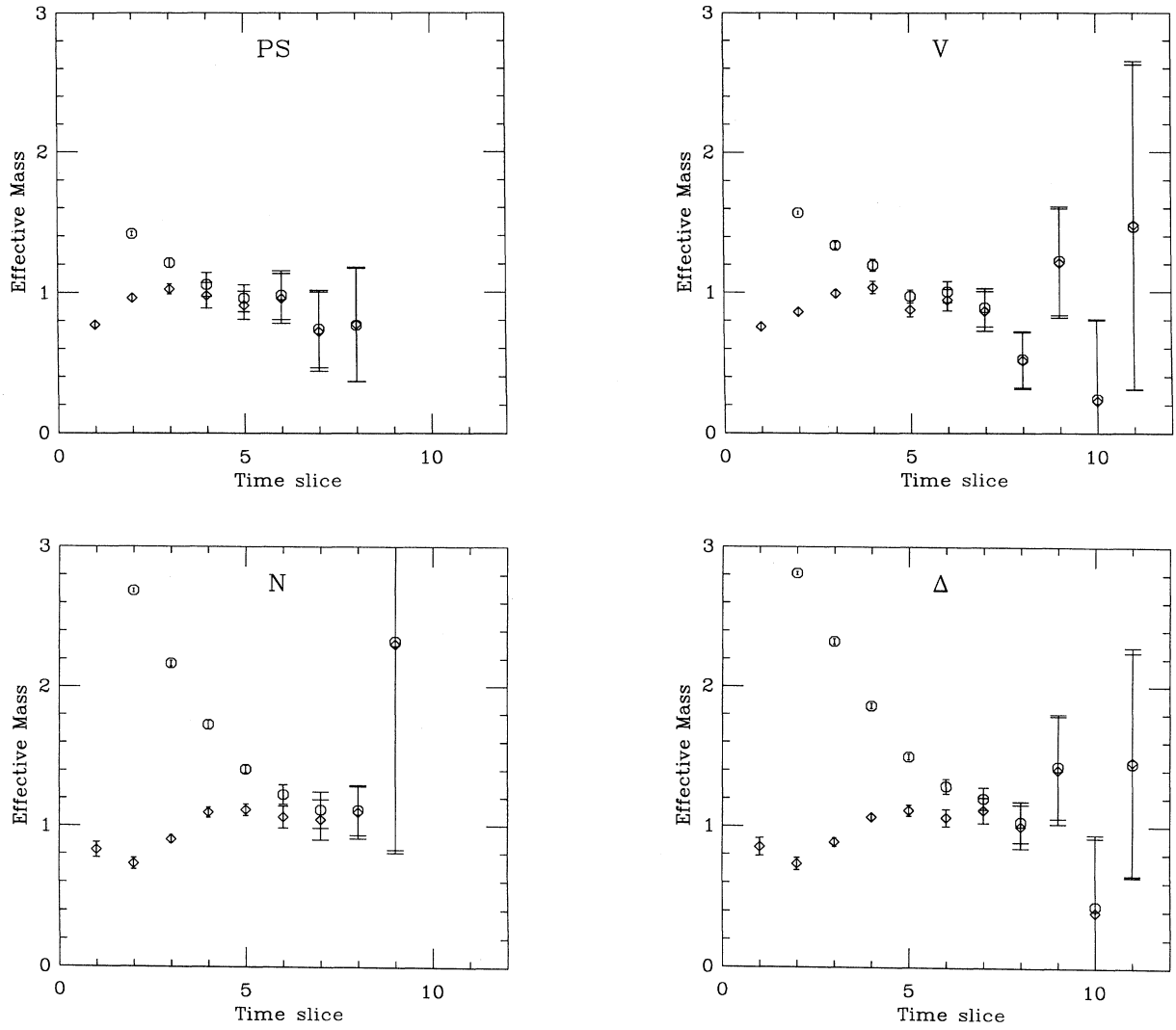

FIG. 6. The effective masses of the first excited states in the pseudoscalar, vector, nucleon, and △ channels, derived from $\lambda_{-}(t,t_0)$ at $t_0=1$ (circles), and from $\chi_{-}(t,\omega)$ at $\omega=0.1\omega_0$ (diamonds).

us to extract the masses of the first excited states. We have explored two methods that yield consistent results. It would be interesting to extend this analysis to a larger basis of operators; such an investigation should lead to appreciably better discrimination of the lowest two states.

ACKNOWLEDGMENTS

This research was supported by the UK Science and Engineering Research Council under Grants No. GR/G 32779, No. GR/H 01069, and No. GR/H 49191, by the University of Edinburgh and by Meiko Limited. We are grateful to Mike Brown of Edinburgh University Computing Service, and to Arthur Trew and Paul Adams of EPCC, for provision and maintenance of service on the Meiko i860 Computing Surface and the Thinking Machines CM-200. C.T.S. and A.D.S. acknowledge the financial support of the UK Science and Engineering Research Council.

[1] R. D. Kenway, in *Proceedings of the XIIth International Conference on High Energy Physics,* Leipzig, East Germany, 1984, edited by A. Meyer and E. Wieczorek (Akademie der Wissenschaften der DDR, Zeuthen, 1984), p. 51.

[2] A. Billoire, E. Marinari, and G. Parisi, Phys. Lett. **162B**, 160 (1985).

[3] APE Collaboration, P. Bacilieri *et al.*, Phys. Lett. B **214**, 115 (1988); Nucl. Phys. **B317**, 509 (1989).

[4] G. Kilcup, in *Lattice '88,* Proceedings of the International Symposium, Batavia, Illinois, 1988, edited by A. S. Kronfeld and P. B. Mackenzie [Nucl. Phys. B (Proc. Suppl.) **9**, 201 (1989)].

[5] T. A. DeGrand and R. D. Loft, Comput. Phys. Commun. **65**, 84 (1991).

[6] F. Butler, in *Lattice '91,* Proceedings of the International

Symposium, Tsukuba, Japan, 1991, edited by M. Fukugita *et al.* [Nucl. Phys. B (Proc. Suppl.) **26**, 287 (1992)].

[7] T. A. DeGrand and M. Hecht, Phys. Lett. B **275**, 435 (1992).

[8] P. B. Mackenzie, in *Lattice '91* [6], p. 369; A. X. El-Khadra, *ibid.*, p. 372.

[9] E. Eichten, in *Lattice '92,* Proceedings of the International Symposium, Amsterdam, The Netherlands, 1992, edited by J. Smit and P. van Baal [Nucl. Phys. B (Proc. Suppl.) **30** (in press)]; H. B. Thacker, *ibid.*

[10] E. Marinari, R. Ricci, and C. Parrinello, in *Lattice '90,* Proceedings of the International Symposium, Tallahassee, Florida, 1990, edited by U. M. Heller, A. D. Kennedy, and S. Sanielevici [Nucl. Phys. B (Proc. Suppl.) **20**, 199 (1991)].

[11] S. Güsken *et al.*, in *Lattice '89,* Proceedings of the International Symposium, Capri, Italy, 1989, edited by R. Petronzio *et al.* [Nucl. Phys. B (Proc. Suppl.) **17**, 361 (1990)]; Phys. Lett. B **227**, 266 (1989).

[12] E. Eichten, G. Hockney, and H. B. Thacker, in *Lattice '89* [11], p. 529.

[13] UKQCD Collaboration, C. R. Allton *et al.*, Phys. Lett. B **284**, 377 (1992).

[14] C. Alexandrou, F. Jegerlehner, S. Güsken, K. Schilling, and R. Sommer, Phys. Lett. B 256 (1991); in *Lattice '91* [6], p. 387.

[15] UKQCD Collaboration, C. R. Allton *et al.*, Edinburgh Report No. 92/507 (unpublished); Liverpool Report No. LTH 301 (unpublished); Southampton Report No. SHEP 92/93-13 (unpublished).

[16] D. Daniel *et al.* Phys. Rev. D **46**, 3130 (1992).

[17] M. Luscher and U. Wolff, Nucl. Phys. **B339**, 222 (1990).

[18] M. Guagnelli *et al.*, in *Lattice '91* [6], p. 278.